



Intradermal drug delivery by nanogel-peptide conjugates; specific and efficient transport of temoporfin



Fatemeh Zabihi^{a,b}, Sebastian Wieczorek^c, Mathias Dimde^a, Sarah Hedtrich^b, Hans G. Börner^{c,*}, Rainer Haag^{a,*}

^a Institute of Chemistry and Biochemistry, Freie Universität Berlin, Takustr. 3, D-14195 Berlin, Germany

^b Institute of Pharmacy (Pharmacology and Toxicology), Freie Universität Berlin, 14195 Berlin, Germany

^c Department of Chemistry, Humboldt-Universität zu Berlin, Laboratory for Organic Synthesis of Functional Systems, Brook-Taylor-Str. 2, D-12489 Berlin, Germany

ARTICLE INFO

Article history:

Received 1 June 2016

Received in revised form 19 July 2016

Accepted 22 July 2016

Available online 25 July 2016

Keywords:

Intradermal delivery

Nanogel

Peptide

Temoporfin

Selective loading

ABSTRACT

Nanogels offer many unique features rendering them as very attractive candidates for drug delivery. However, for their applications the loading capacity and specific encapsulation, in particular for hydrophobic drugs, in a complex media are two critical factors. In this work, we report for the first time on the preparation of nanogel-peptide conjugates with the ability of specific encapsulation of temoporfin (*m*-THPC). The peptide was selected based on combinatorial means and it was conjugated to polyglycerol as the nanogel precursor. We observed that the loading capacity of nanogels improved 16 times upon peptide conjugation. Skin penetrations tests in barrier deficient skin showed that nanogel-peptide conjugates enhance the penetration of *m*-THPC in the viable skin layers efficiently. This study indicates that nanogel-peptide conjugates could be used as unique carriers with high loading capacity for hydrophobic compounds, which provides the basis for the design of advanced topical drug delivery systems.

© 2016 Elsevier B.V. All rights reserved.

1. Introduction

Skin is the outermost organ of the human body with the main task to protect it from excessive water loss and the entry of foreign material [1]. Moreover, skin is an interesting alternative route for drug administration [2], particularly when skin is the target organ [1–3]. The outermost layer of the human skin, the stratum corneum, which consists of corneocytes and a tightly packed lipid matrix, does not allow for efficient dermal absorption of compounds with molecular weights higher than 500 Da [4]. To overcome these limitations and facilitate the diffusion of desirable compounds into the skin, assistant materials such as nanocarriers can be used.

Photodynamic therapy, a treatment method based on nontoxic photoactive agents, is widely used for the treatment of human skin cancer [5,6]. Following activation using visible light, reactions between the photosensitizer in the excited state with the oxygen inside of living cells or tissues result in the formation of reactive oxygen species which destroy cell compartments and induce cell death. Temoporfin (*meta*-tetra(hydroxyphenyl)chlorin, *m*-THPC) is a highly lipophilic, second generation photosensitizer and mainly used for the photodynamic therapy of skin cancer [7]. The poor-water solubility of this compound is a major drawback that limits its bioavailability. Moreover, its molecular weight of ~680 Da restricts efficient skin penetration which is only observed for compounds ≤500 Da.

Nanogel particles with unique properties such as high drug loading, stability in physiological media, and stimulus-triggered release of loaded drugs appears to be attractive candidates for the use in intra- and transdermal drug delivery [8–11]. Nanogels are nanosized polymeric networks in which building blocks are physically or chemically cross-linked [12]. They have recently shown high potential to load and deliver photosensitizers [13,14]. Since nanogels are highly hydrophilic in nature, they do not efficiently encapsulate hydrophobic guest molecules such as *m*-THPC. To overcome this obstacle, incorporation of hydrophobic segments into the backbone of nanogels might be a suitable strategy [15]. Tunable hydrophobicity of nanogels by stimuli factors e.g. temperature has been used successfully to control release of encapsulated guest molecules in the target tissues [9,16]. However, toxicity of the incorporated hydrophobic segments in the backbone of nanogels and their adverse effect on the normal tissues often remains a challenging issue, which has to be considered. Specific interaction, however, would enable discrete binding of the cargo drug to the nanogel transporter, which has been identified as another relevant factor to realized advanced drug delivery systems. Particularly, in the complex environment of the biological media, specific interactions might reduce undesirable co-transport of other entities from the biosystem to consequently improve the efficiency of these nanocarriers and avoid adverse effects.

Börner et al. recently have described a method based on combinatorial means to identify peptide sequences for specific interactions with small organic drug entities such as kinase inhibitors or photosensitizers like *m*-THPC [17,18]. While peptide-*block*-polymer conjugates proved

* Corresponding authors.

E-mail address: haag@chemie.fu-berlin.de (R. Haag).

the potentials for different biomedical applications [19–24], the integration of drug specific binders in peptide-*block*-polymer conjugates provides new opportunities to generate drug delivery systems with precisely tunable interaction capabilities and physiological properties [25,26].

In this work we have applied this concept to nanogels for rendering *m*-THPC water soluble by specific host guest interactions, leading to drug delivery systems with adjustable release profiles improved delivery efficiency and desirable barrier translocation. A peptide suitable for sequences specific interaction with *m*-THPC has been selected based on previously reported work [18], and it was conjugated to hyperbranched polyglycerol as a precursor of nanogels. After precursor crosslinking, nanogel-peptide conjugates with different peptide ratios and abilities to load *m*-THPC were obtained and characterized. The effects of the peptides on the loading capacity, the specificity of the interactions with *m*-THPC and the release profiles as well as size and morphology of nanogels have been investigated.

2. Experimental

2.1. Materials and methods

Hyperbranched polyglycerol (hPG) was synthesized by anionic ring opening polymerization of glycidol using potassium-*tert*-butoxide as initiator [27]. Dimethylformamide (DMF), acetone, phosphate buffered saline (PBS), Traut's reagent, triethylamine (TEA), acryloyl chloride, 1-ethyl-3-(3-dimethylaminopropyl)carbodiimid (EDCI), and 1-hydroxybenzotriazol (HOBt) were purchased from Sigma-Aldrich. *m*-THPC was provided kindly by Professor Mathias O. Senge (School of Chemistry, SFI Tetrapyrrole Laboratory, Trinity College Dublin, Ireland). Water was used from Milli-Q® Advantage A10 Water Purification System in all experiments. Phosphate-buffered saline (PBS) (10×) pH 7.4 (ThermoFisher Scientific) was diluted 10 times with Milli-Q water. Benzoylated cellulose dialysis tubes (width: 32 mm, MWCO >1000–2000 g/mol) from Sigma-Aldrich were used for purification of the synthesized compounds. The peptide with Ac-QFFLFFQGG-COOH sequence was taken from reference [18], briefly *N*-α-Fmoc protected amino acids Fmoc-Gly-OH, Fmoc-Gln(Trt)-OH, Fmoc-Leu-OH, Fmoc-Phe-OH were purchased from IRIS Biotech GmbH (Marktredwitz, Germany). 2-(1H-benzotriazole-1-yl)-1,1,3,3-tetramethyluronium-hexafluorophosphate (HBTU) and *N*-methyl-2-pyrrolidone (NMP, 99.9 + %, peptide synthesis grade) were used as received from IRIS Biotech GmbH. *N,N*-diisopropylethylamine (DIPEA; Acros, peptide grade), piperidine (Acros, peptide grade) and triethylsilane (TES; Alfa Aesar, Karlsruhe, Germany, 98 + %) have been used as received. Trifluoroacetic acid (TFA; Acros, peptide grade) was distilled prior to use. Dichloromethane (DCM, IRIS Biotech GmbH, peptide grade) was distilled from CaH₂ prior to use. Chlorotriyl chloride resin was obtained from IRIS Biotech GmbH.

2.2. Synthesis of the peptide

Peptide (Ac-QFFLFFQGG-COOH) for nanogel conjugation was obtained by automated solid-phase peptide synthesis on an ABI 433a peptide synthesizer (Applied Biosystems, Foster City, CA 94404, USA) following standard *ABI-Fastmoc* protocol (single coupling) with NMP as solvent. As solid support, Chlorotriyl chloride resin preloaded with 0.5 mmol/g Fmoc-Gly-OH was used. After stepwise polypeptide assembly via HBTU/NMP/piperidine protocol, the peptide was cleaved from the solid support by treatment with a mixture of 97% TFA, 2% TES and 1% water at room temperature for 3 h. The resin was filtered, washed with TFA and the collected supernatants were concentrated in vacuo. Afterwards, the peptide was precipitated in cold diethyl ether, centrifuged (20 min., 9000 rpm) and the supernatants were removed by decantation. Residues were dissolved in 2 mL TFA and precipitated again in cold diethyl ether (see above). This procedure was repeated two

times and precipitates were dried in vacuo. To remove TFA, the peptide was finally freeze-dried from water/DMSO mixture (50:50 v/v).

2.3. Synthesis of polyglycerol-peptide conjugate (hPG-Pep)

For preparation of hPG having two peptide chains (hPG-Pep₂), polyglycerol with 10% amino functional groups (hPG-NH₂) (20 mg, 19×10^{-4} mmol) and peptide with Ac-QFFLFFQGG-COOH sequence (6.1 mg, 5.9×10^{-3} mmol) were dissolved in dry DMF (4 and 6 mL, respectively) in different reaction flasks. Then triethylamine (TEA) (7.4 μL, 5.3×10^{-5} mmol) was added to the peptide solution and it was stirred at 0 °C for 30 min. 1-hydroxybenzotriazol (HOBt) (7.2 mg, 5.3×10^{-2} mmol) and 1-ethyl-3-(3-dimethylaminopropyl)carbodiimid (EDCI) (10.4 mg, 5.4×10^{-2} mmol) were also dissolved in dry DMF (2 mL) in another reaction flask. Those solutions were simultaneously added dropwise to the stirring solution of hPG-NH₂ under argon atmosphere. Then mixture was stirred at room temperature overnight. The solvent was evaporated to reach 50% of the original volume of solution and the mixture was transferred to a dialysis bag (2 kDa MWCO) and dialyzed against Milli-Q water for 3 days. Afterwards, the mixture was centrifuged for 20 min at 5000 rpm in order to remove traces of unreacted peptides and undissolved products and the supernatant was concentrated to 3 mL. The product was lyophilized and the weight of final product was 18.5 mg (93% yield). For preparation of polyglycerol with three peptide chains (hPG-Pep₃), a higher amount of peptide (9.5 mg, 8.3×10^{-3} mmol) was used in the same synthetic protocol.

2.4. Synthesis of acrylated polyglycerol (hPG-Acr)

Acrylation of hPG was carried out according to the previously reported work [28]. Briefly, hPG was dried overnight at 50 °C under high vacuum (542 mg, 0.0437 mmol) and subsequently it was dissolved in dry DMF (2.5 mL). Triethylamine (TEA, 109.08 mg, 1.078 mmol) was added to the solution, after cooling down to 0 °C. Acryloyl chloride (88.6 mg, 0.98 mmol) was dissolved in dry DMF (2.5 mL) at 0 °C and added dropwise to the cold solution of hPG under argon atmosphere. Then the ice bath was removed and the reaction was stirred at room temperature overnight. The reaction mixture was concentrated under high vacuum, transferred to a dialysis bag (2 kDa MWCO) and dialyzed against Milli-Q water for three days. Number of acrylate groups conjugated to hPG was determined 10% by ¹H NMR.

2.5. Thiolation of hPG-Pep

2-Iminoethiolane hydrochloride (Traut's reagent) was used to convert amino functional groups of hPG-Pep to thiols. In this procedure hPG-Pep (2.5 mg) was mixed with Traut's reagent (0.48 mg) in a slightly acidic aqueous solution (500 μL Milli-Q water). Then, *tris*(2-carboxyethyl)phosphine (5 μL) was added to the mixture. The product of this reaction was used for the preparation of nanogels without further purification.

2.6. Preparation of nanogels using Thio-Michael nanoprecipitation method

By this method, nanogels with different composition and in the range of 100–1000 nm sizes were synthesized. hPG and hPG-Pep with thiol groups were used for the synthesis of nanogels without and with peptide chains, respectively. A cold aqueous solution of already prepared thiolated hPG or hPG-Pep (2.5 mg in 500 μL Mill-Q water) was mixed with the cold aqueous solution of hPG-Acr (2.5 mg in 500 Milli-Q water μL). The obtained solution was then injected into 20 mL acetone as nonsolvent, while it was slowly stirred at room temperature for 3 min. Then it was left (without stirring) at room temperature for 3 h. Afterwards, 2-hydroxyethyl acrylate (0.725 μL) was added to the mixture as quenching reagent. The resulting mixture was left without stirring at room temperature overnight. Applying vacuum, acetone was

removed from the mixture and remained solution was transferred to a dialysis bag (50 kDa MWCO) and dialyzed against Milli-Q water for 24 h. Sizes of nanogels were adjusted by manipulation of the concentration of precursors and amount of acetone. Nanogels with bigger sizes were obtained when concentration of precursors of the nanogel was decreased and volume of acetone in the synthetic protocol was increased.

2.7. Loading of nanogels with *m*-THPC

Nanogels were loaded with *m*-THPC using a thin film method.

In this method, *m*-THPC (2 mg) was dissolved in ethanol (1 mL) and solution was stirred for 1 h at room temperature. Then solvent was evaporated at room temperature and a thin layer of drug was produced. Afterwards, aqueous solution of the nanogel (2 mg/mL) it was applied to this thin film. The solution was stirred (1200 rpm) at room temperature for 48 h and then the sample was filtered through a 0.45 μm syringe filter to remove *m*-THPC. UV absorption of an aqueous solution of nanogels loaded by *m*-THPC was recorded and concentration of *m*-THPC was calculated according to the calibration curve of the free drug. The loading capacity of nanogels was obtained by dividing the weight of the loaded drug by the initial weight of nanogels.

2.8. Selectivity of hPG-Pep nanogels with respect to *m*-THPC loading

This experiment is similar to loading of *m*-THPC by nanogels as described before but a mixture of *m*-THPC (1 mg/mL) and pyrene (1 mg/mL) was used in thin film loading procedure. After 72 h sample was filtered through a 0.45 μm syringe filter and loading capacity of nanogel was calculated using UV absorption spectroscopy.

2.9. Release of loaded *m*-THPC from nanogels

An aqueous solution of nanogel loaded with *m*-THPC (1 mL/mg) was purified cellulose membrane dialysis tubing. The membrane was transferred into a flask containing 10 mL of PBS (pH 7.4) and Igepal CA-630 (2% v/v). Temperature was set at 32 °C and the solution was stirred continuously at 500 rpm. Sample (1 mL) was withdrawn after 60 min, 120 min, 240 min, 300 min, 360 min, 420 min, 480 min, 540 min, 600 min, 1080 min, 1440 min, 1800 min and replaced with equal volumes of the fresh buffer. The quantity of released drug was analyzed by a UV spectrophotometer and determined from the calibration curve obtained previously under the same conditions.

2.10. Skin penetration studies

To characterize the dermal drug delivery efficiency of nanogels, the skin absorption of loaded *m*-THPC was evaluated by validated test procedures using the Franz cell set-up and picture analysis [29,30]. *m*-THPC (0.13% w/w) loaded nanogels and *m*-THPC-loaded conventional base cream were tested in parallel using excised human skin of the same donor [29]. *m*-THPC incorporated into base cream (0.13% w/w) served as reference [31]. Prior to the experiment, human skin was thawed and discs of 2 cm diameter were punched and mounted onto static-type Franz cells (diameter 15 mm, volume 12 mL, PermeGear Inc., Bethlehem, PA, USA) with the horny layer facing the air and the dermis having contact with the receptor fluid phosphate buffered saline pH 7.4 (PBS, 33.5 °C, skin surface temperature about 32 °C) stirred at 500 rpm. After 30 min, 36 μL of the test formulations and reference cream was applied onto the skin surface (finite-dose approach) and remained there for 6 h. Subsequently, the skin was removed from the Franz cells, and the skin surface was gently cleaned. Afterwards, treated skin areas were punched, embedded in tissue freezing medium (Jung, Nussloch, Germany) and stored (Polyscience, Eppelheim, Germany) at

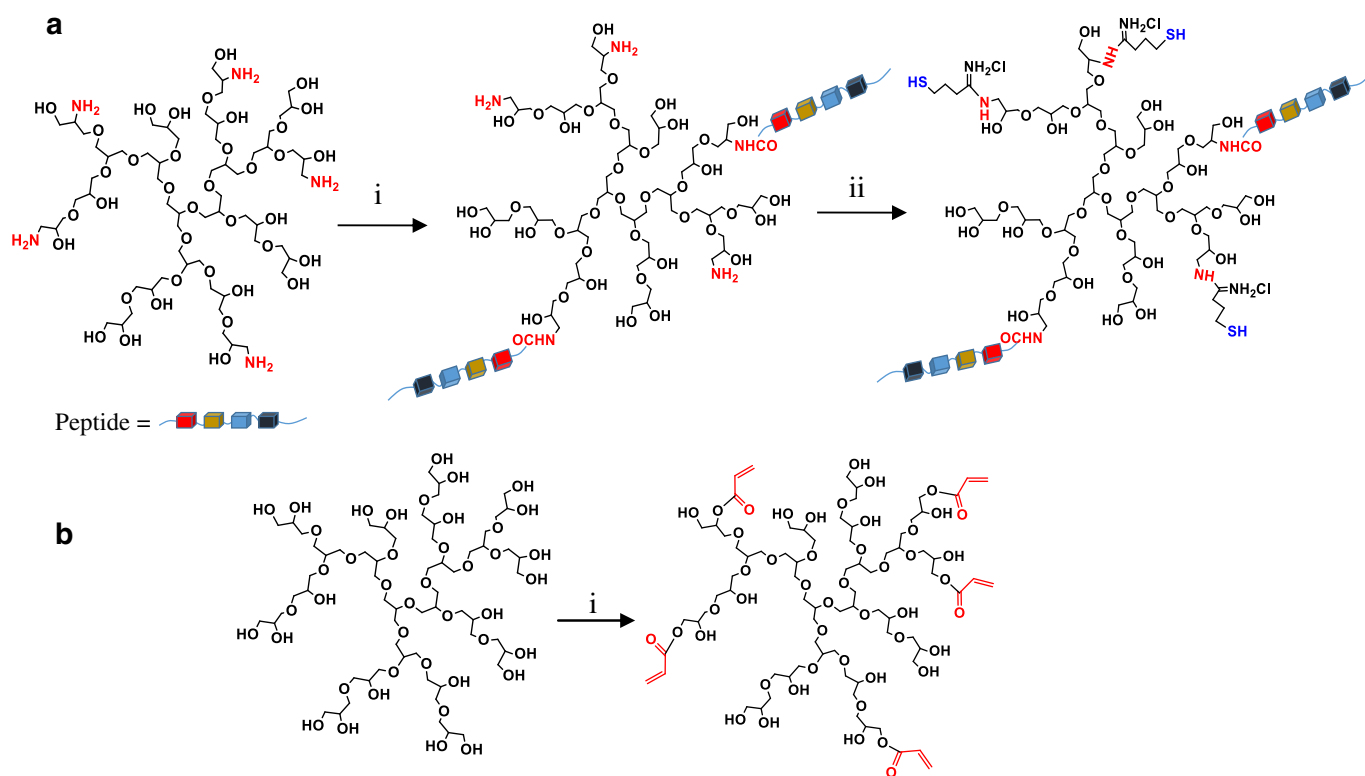


Fig. 1. (a) Schematic representation of conjugation of peptide chains to hPG-NH₂ and consequently thiolation of hPG-Pep. Thiol groups are reactive functional groups for the crosslinking process in the nanogel preparation process. i) DMF, TEA, Peptide-COOH, EDCl, HOBT, r.t., 12 h. ii) 2-Iminothiolane (Traut's reagent), H₂O, r.t., 20 min. (b) Acrylation of hPG by reaction between acryloyl chloride and hydroxyl functional groups of polyglycerol. i) DMF, Acryloyl chloride, TEA, 0 °C- r.t., overnight.

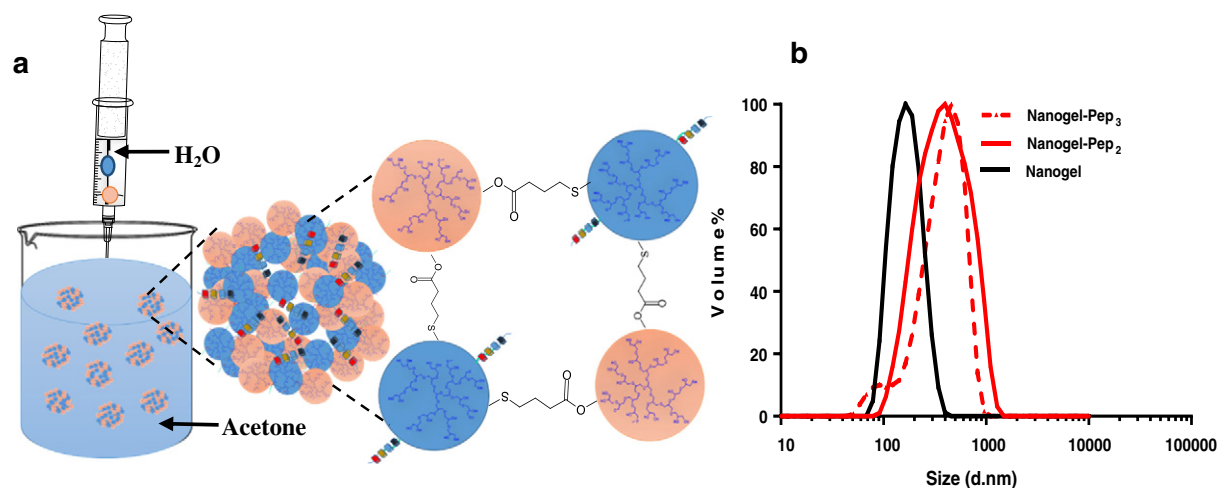


Fig. 2. (a) Preparation of nanogels having peptide chains in their structure by nanoprecipitation. (b) DLS diagrams of nanogels without and with peptide segments. Conjugation of peptide segments to the nanogels increase their sizes compared to peptide-free analogue.

a temperature of -80°C . To determine *m*-THPC penetration, the skin discs were cut into vertical slices of $10\ \mu\text{m}$ thickness using a freeze microtome (Frigocut 2800 N, Leica, Bensheim, Germany). The slices were subjected to normal light and fluorescence light. *m*-THPC distribution was visualized by fluorescence microscopy (excitation: $560\text{--}540\ \text{nm}$, emission: $630\text{--}660\ \text{nm}$).

To induce barrier-impaired skin, 50 times tape-stripping was performed prior to the penetration studies.

3. Result and discussion

The nanogel-peptide conjugates were synthesized by crosslinking of precursor polymers. These consisted of hyperbranched polyglycerols functionalized with peptides (hPG-Pep) as prepared by reaction between amino functional groups of hPG-NH₂ and terminal carboxyl group of peptide segments (Fig. 1).

The number of peptide segments per polyglycerol was adjusted to be 2/1 or 3/1 (hPG-Pep₂ or hPG-Pep₃, respectively) to improve the loading capacity, achieve specific interactions of hPG-Pep toward *m*-THPC and preserve its water solubility. hPG-Pep compounds were characterized by IR and NMR spectroscopic methods. In the IR spectra of these compounds an absorbance band at $1634\ \text{cm}^{-1}$ could be assigned to the carbonyl groups of the peptides, in addition to the characteristic bands of the polyglycerol at $1333\ \text{cm}^{-1}$ (C—O) and $3372\ \text{cm}^{-1}$ (O—H) indicating conjugation of peptide segments to the amino functional groups of polyglycerol (Fig. S3). In the ¹H NMR spectra of hPG-Pep compounds, signals at 6.9–7.4 and 0.85–1.5 ppm correspond to the aromatic and aliphatic protons of the side chains groups of peptide, respectively. Also characteristic signals for the aliphatic protons of polyglycerol are present at 3.2–4.1 ppm (Fig. S4).

The average number of conjugated peptide segments to polyglycerol was determined from ¹H NMR spectra by comparing the ratio of the integral intensities from aromatic proton resonances of the peptide with

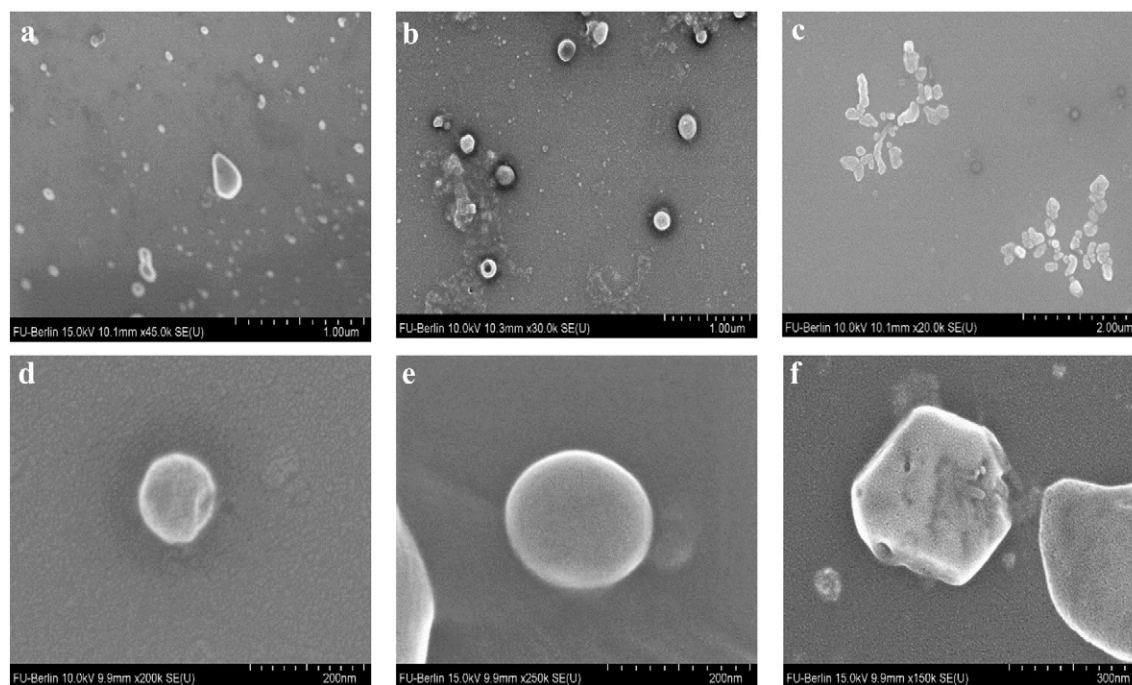


Fig. 3. (a) SEM image of nanogels without peptide chains. (b and c) SEM images of nanogel-Pep₂ and nanogel-Pep₃, respectively. (d) SEM image of nanogel without peptide chains with higher magnification. (e and f) SEM images of nanogel-Pep₂ and nanogel-Pep₃, respectively, with higher magnification.

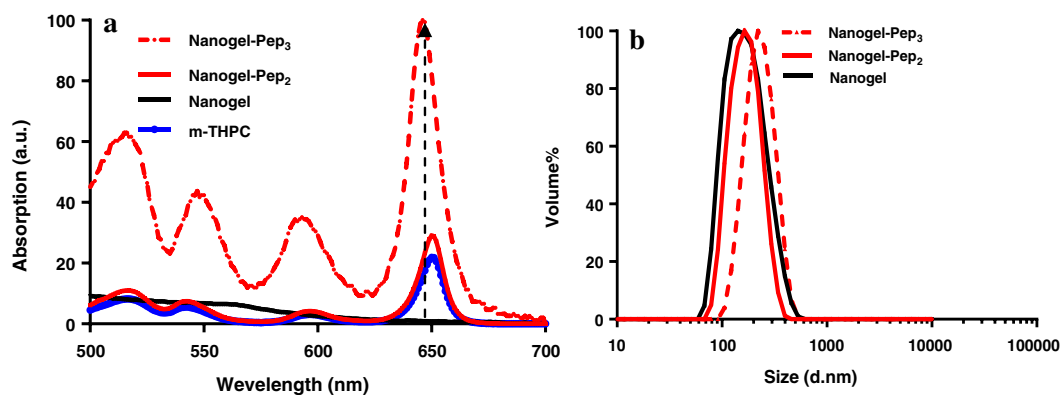


Fig. 4. (a) UV absorption spectra of *m*-THPC solubilized by nanogel without peptide, nanogel-Pep₂ and nanogel-Pep₃. (b) DLS diagrams of nanogels with and without peptide chains after drug loading.

that one of the characteristic resonances from polyglycerol (Fig. S4). In order to activate hPG-Pep for the thiol-click reaction, the non-reacted amino functionalities of this compound were thiolated via the Traut's reagent (Fig. 1a).

The hPG containing acryloyl segments (hPG-Acr), which is a precursor for the alternative preparation route of nanogels, was accessed by reaction between hydroxyl functionalities of polyglycerol and acryloyl chloride (Fig. 1b). The number of acrylated hydroxyl groups was determined to be 10% according to the ¹H NMR spectra of the product (Fig. S5).

The goal of this research work was to investigate the effects of peptides on interactions between nanogels and *m*-THPC to increase the loading capacity as well as establish specific interactions toward this

therapeutic agent. Therefore, for each nanogel-peptide conjugate, its analogue without peptides was synthesized and characterized and their interactions with *m*-THPC were investigated in a comparative study. The peptide loaded nanogels as well as the peptide free nanogel controls were prepared by in situ thiol-click reaction in the nano-precipitation process by using similar conditions (Fig. 2a). The nanogel-peptide conjugates synthesized using hPG-Pep₂ and hPG-Pep₃ were referred to as nanogel-Pep₂ and nanogel-Pep₃, respectively. Sizes and morphologies of the nanogels were evaluated by DLS and SEM measurements.

Fig. 2b shows DLS diagram of nanogel-peptide conjugates and their analogues without peptides as control. Obviously, the size of nanogel-peptide conjugates is larger than their analogous without peptide

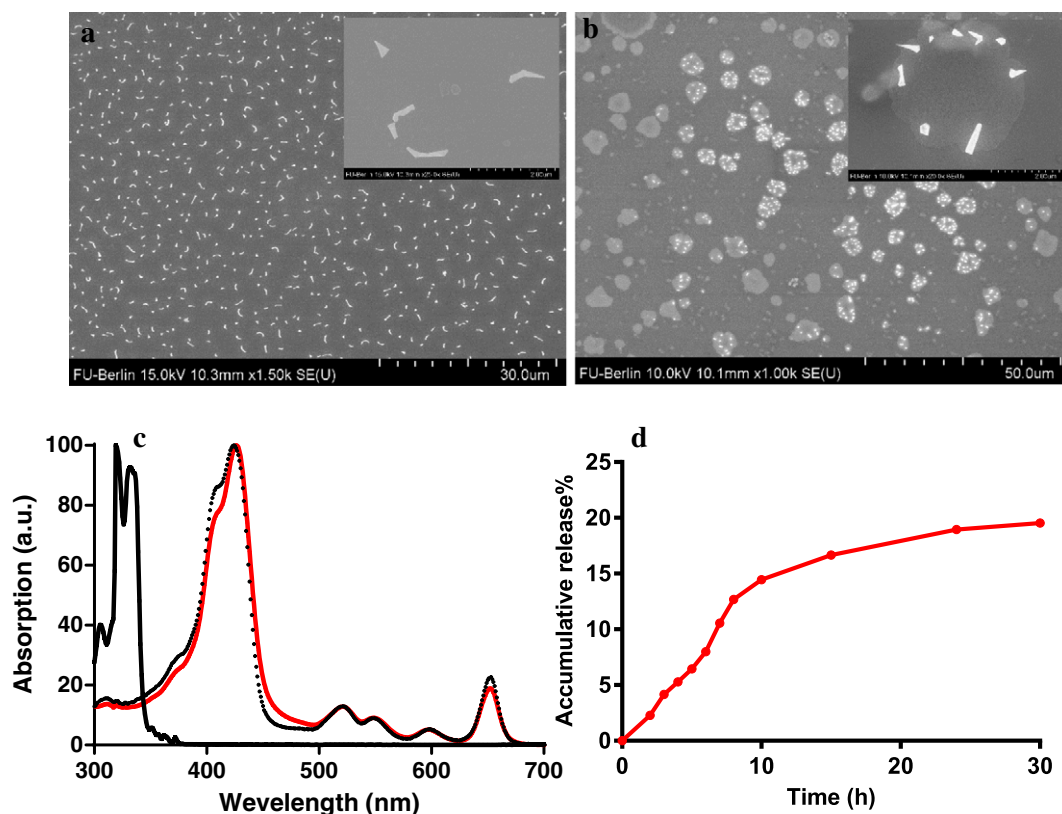


Fig. 5. (a and b) SEM images of nanogel-Pep₂ and nanogel-Pep₃, respectively with the loaded *m*-THPC. (c) Selective encapsulation of *m*-THPC when nanogel-Pep₂ is incubated with a mixture of pyrene and *m*-THPC guest molecules after 72 h. UV spectra of *m*-THPC and pyrene before incubation with nanogels (black dash and solid lines, respectively) and after incubation and purification (red line). Clearly nanogels show a high affinity toward *m*-THPC, while pyrene cannot be recognized within the limit of detection. (d) Release profile of *m*-THPC from nanogel-peptide conjugate at pH 7.4 and 32 °C.

functionalization. This is probably due to the hydrophobic interactions between peptides of nanogels in aqueous solutions followed by nanogel aggregation. Based on the DLS data, the average size of the peptide free nanogel, nanogel-Pep₂ and nanogel-Pep₃ are 180 nm, 350 nm and 400 nm, respectively. The size of the nanogel-Pep₃ is bigger than nanogel-Pep₂, due to the higher number of peptide chains.

SEM images show a spherical morphology for nanogels of the peptide free controls (Fig. 3a and d). However, nanogel-peptide conjugates aggregated in the most cases (Fig. 3b–3f). The increased sizes and tendency to assemble of nanogel-peptide conjugates is most likely due to the hydrophobic interactions between peptides in an aqueous environment (Fig. S6a and S6b). Fig. 3c and f show SEM images of nanogel-Pep₃. In these images nanogels are interacting and creating bigger aggregates.

After characterization, nanogels were subjected to be loaded with *m*-THPC as a guest molecule. The drug payload capacity of nanogel-peptide conjugates was significantly increased compared to the peptide free controls and it was strongly depended on the degree of peptide functionalization of the nanogels. While the loading capacity of nanogels without peptides was 3.7 mg/g, it increased to 25 mg/g and 61 mg/g for nanogel-Pep₂ and nanogel-Pep₃, respectively. Therefore, conjugation of 2 and 3 peptides per hPG precursor improves the loading capacity of the crosslinked nanogels 7 and 16 times, respectively, compared to their analogues without peptide functionalization (Fig. 4a).

An indirect evidence for interactions between peptides and *m*-THPC is the decreasing size of nanogel-peptides upon interaction with the hydrophobic drug (Fig. 4b) compared to the DLS measurements of nanogels without drug loading (Fig. 2b). According to DLS data the average size of the peptide free nanogel, nanogel-Pep₂ and nanogel-Pep₃ after loading with *m*-THPC are 160 nm, 200 nm and 300 nm, respectively. Guest molecules interact with the peptide functionalities of the

nanogels, reducing peptide-peptide interactions in-between other nanogels. This would result in the dissociation of the nanogel aggregates. As a control, size of nanogels without peptide chains did not change significantly after loading of *m*-THPC (Fig. 4b).

SEM images show that morphology of the nanogel-peptide has changed dramatically upon loading of *m*-THPC (Fig. 5a and b). Due to the crystalline guest molecules, the electron contrast of those *m*-THPC loaded nanogels is apparently higher than that of the non-loaded controls.

The aggregation of nanogels can be observed in the case of nanogel-Pep₃, which is due to the higher degree of functionalization with peptides and their interactions even after loading with guest molecules.

Since the peptide was selected for drug binding and specific interaction with *m*-THPC, the ability of nanogel-Pep to load this guest molecule in a more complex media was investigated. Nanogel-Pep₂ was incubated with a mixture of pyrene and *m*-THPC and the amount of guest molecules loaded to the nanogel was evaluated by UV absorption spectroscopy. Pyrene was used as a model compound, representing numerous small water insoluble entities present in a complex biological system. Surprisingly it was found, that nanogel-Pep₂ loaded *m*-THPC selectively from the mixture, whereas pyrene was disregarded (Fig. 5c). This indicates that the nanogel-peptide conjugates bind specifically and other entities in the complex media, improved delivery of the loaded therapeutic agents and reduced unfavored transport of biological entities.

In vitro release of *m*-THPC from nanogel-peptide conjugates was investigated and only 15–20% of drug was released after 24 h. The slow release of the encapsulated drug molecules is probably due to strong interactions with the peptide chains of nanogels. This results in a high affinity between encapsulated drug molecules and nanogels and

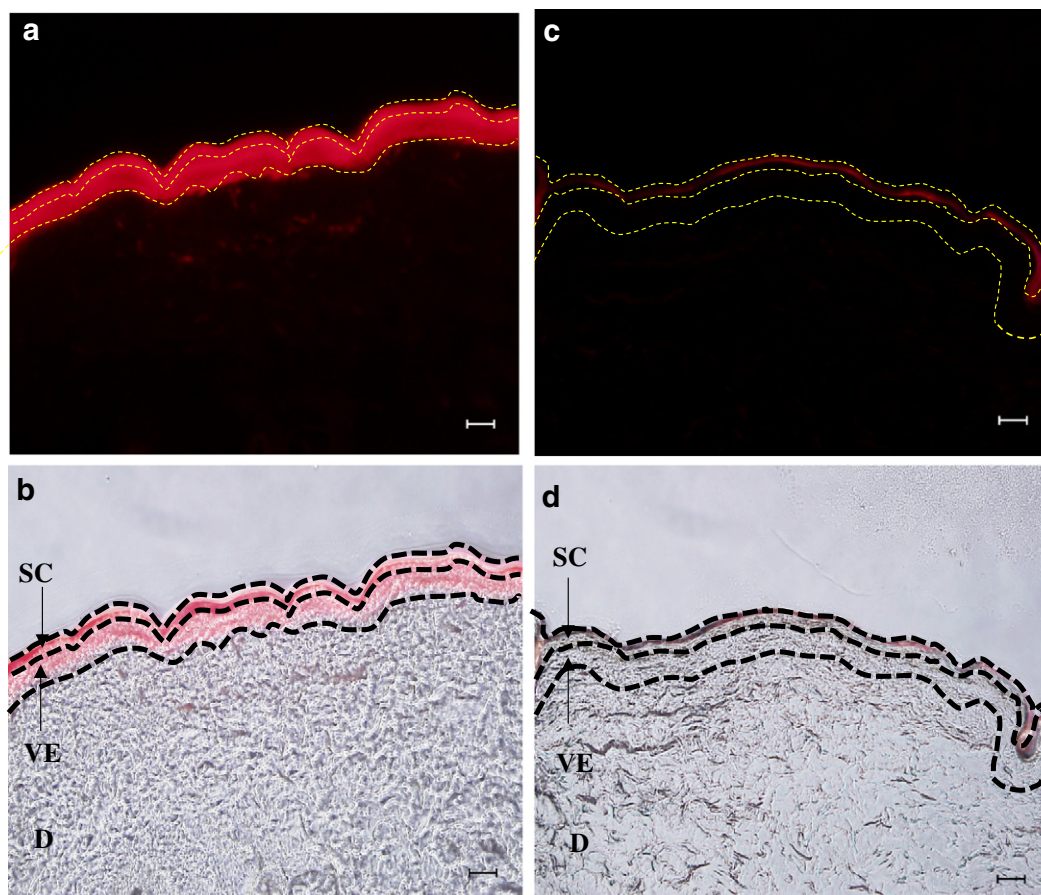


Fig. 6. Representative fluorescence and bright field microscopy images of tape stripped human skin after topical application of (a and b) *m*-THPC loaded (0.13%) nanogel-Pep₂ and (c and d) conventional base cream containing 0.13% *m*-THPC. (SC = stratum corneum, VE = viable epidermis, D = dermis.) Scale bar 50 μm.

therefore hampering fast release. The slow rate of release potentially increases the bioavailability of drug molecules and decrease their adverse effect on the living organs (Fig. 5d).

In order to investigate the ability of the synthesized nanogel-Pep carriers to transport *m*-THPC into normal and tape stripped human skin, the skin penetration of *m*-THPC loaded nanogels-Pep₂ was evaluated. While the amount of the penetrated dye into the normal skin was not considerable (Fig. S7), fluorescence microscopy evaluation showed that nanogel-Pep₂ significantly enhanced the uptake of *m*-THPC in the viable epidermis and even in deeper dermal layer of the tape stripped skin (Figs. 6a). In contrast, *m*-THPC was exclusively detected in the stratum corneum following application of the conventional base cream (Fig. 6b). The ability of nanogel-Pep₂ to enhance dermal delivery of *m*-THPC is due to the amphiphilicity of this carrier originating from hydrophobic peptides and hydrophilic nanogel.

High skin penetration, specific and high loading capacity together with slow release of drug are superior advantages for peptide based drug delivery systems.

4. Conclusion

Nanogel-peptide conjugates with unique properties constitute novel drug delivery systems into the skin. Incorporation of peptide segments in the structure of polyglycerol based nanogels dramatically increased the loading capacity as well as the binding specificity of the carrier with the target therapeutic agents. The peptides also modify other physicochemical properties of nanogels such as their, solubility, size and morphology. Due to a sequence specific interaction with the encapsulated drug molecules, peptides induce a slow release profile for the drug-loaded nanogel-peptide conjugates. Preliminary skin penetration tests showed efficient dermal delivery of *m*-THPC by nanogel carriers, whereas free *m*-THPC is restricted from skin absorption due to the high molecular weight of the drug entity.

Acknowledgment

We would like to thank the German Science Foundation within SFB 1112 for financial support and the core-facility Biosupramol for analytical measurements. HGB acknowledges funding by the European Research Council under the European Union Seventh Framework Programme (FP07-13)/ERC Starting grant "Specifically Interacting Polymers – SIP" (ERC 305064). Also we would like to thank Dr. Florian Paulus, Cathleen Schlesener and Stefan Hönzke for their kindly collaboration to synthesize polyglycerol, polyglycerolamine and for introducing Franz cell to the skin penetration experiments.

Appendix A. Supplementary data

Supplementary data to this article can be found online at <http://dx.doi.org/10.1016/j.jconrel.2016.07.033>.

References

- [1] M.-A. Bolzinger, S. Briçonnet, J. Pelletier, Y. Chevalier, Penetration of drugs through skin, a complex rate-controlling membrane, *Curr. Opin. Colloid Interface Sci.* 17 (2012) 156–165.
- [2] M.R. Prausnitz, R. Langer, Transdermal drug delivery, *Nat. Biotechnol.* 26 (2008) 1261–1268.
- [3] K. Higaki, M. Asai, T. Suyama, K. Nakayama, K.-i. Ogawara, T. Kimura, Estimation of intradermal disposition kinetics of drugs: II. Factors determining penetration of drugs from viable skin to muscular layer, *Int. J. Pharm.* 239 (2002) 129–141.
- [4] Y. Chen, P. Quan, X. Liu, M. Wang, L. Fang, Novel chemical permeation enhancers for transdermal drug delivery, *Asian Journal of Pharmaceutical Sciences* 9 (2014) 51–64.
- [5] D.E.J.G.J. Dolmans, D. Fukumura, R.K. Jain, Photodynamic therapy for cancer, *Nat. Rev. Cancer* 3 (2003) 380–387.
- [6] K. Trauner, R. Gandour-Edwards, M. Bamberg, N.S. Nishioka, T. Flotte, S. Autry, T. Hasan, Influence of light delivery on photodynamic synovectomy in an antigen-induced arthritis model for rheumatoid arthritis, *Lasers Surg. Med.* 22 (1998) 147–156.
- [7] V. Reshetov, H.-P. Lassalle, A. François, D. Dumas, S. Hupont, S. Gräfe, V. Filipe, W. Jiskoot, F. Guillemin, V. Zorin, L. Bezdetsnaya, Photodynamic therapy with conventional and PEGylated liposomal formulations of mTHPC (temoporfin): comparison of treatment efficacy and distribution characteristics in vivo, *Int. J. Nanomedicine* 8 (2013) 3817–3831.
- [8] Y. Jiang, J. Chen, C. Deng, E.J. Suuronen, Z. Zhong, Click hydrogels, microgels and nanogels: emerging platforms for drug delivery and tissue engineering, *Biomaterials* 35 (2014) 4969–4985.
- [9] M. Witting, M. Molina, K. Obst, R. Plank, K.M. Eckl, H.C. Hennies, M. Calderón, W. Friess, S. Hedtrich, Thermosensitive dendritic polyglycerol-based nanogels for cutaneous delivery of biomacromolecules, *Nanomedicine: nanotechnology, biology, and medicine* 11 (2015) 1179–1187.
- [10] M. Simphiwe, M. Thashree, E.C. Yahya, K. Pradeep, C.d.T. Lisa, P. Viness, A review of polymeric colloidal nanogels in transdermal drug delivery, *Curr. Pharm. Des.* 21 (2015) 2801–2813.
- [11] M. Toyoda, S. Hama, Y. Ikeda, Y. Nagasaki, K. Kogure, Anti-cancer vaccination by transdermal delivery of antigen peptide-loaded nanogels via iontophoresis, *Int. J. Pharm.* 483 (2015) 110–114.
- [12] R.T. Chacko, J. Ventura, J. Zhuang, S. Thayumanavan, Polymer nanogels: a versatile nanoscopic drug delivery platform, *Adv. Drug Deliv. Rev.* 64 (2012) 836–851.
- [13] J.-Y. Kim, W.I. Choi, M. Kim, G. Tae, Tumor-targeting nanogel that can function independently for both photodynamic and photothermal therapy and its synergy from the procedure of PDT followed by PTT, *J. Control. Release* 171 (2013) 113–121.
- [14] F. Schmitt, L. Lagopoulos, P. Käufer, N. Rossi, N. Busso, J. Barge, G. Wagnières, C. Laue, C. Wandrey, L. Juillerat-Jeanneret, Chitosan-based nanogels for selective delivery of photosensitizers to macrophages and improved retention in and therapy of articular joints, *J. Control. Release* 144 (2010) 242–250.
- [15] T. Fernandes Stefanello, A. Szarpak-Jankowska, F. Appaix, B. Louage, L. Hamard, B.G. De Geest, B. van der Sanden, C.V. Nakamura, R. Auzély-Velty, Thermoresponsive hyaluronic acid nanogels as hydrophobic drug carrier to macrophages, *Acta Biomater.* 10 (2014) 4750–4758.
- [16] H. Yang, Q. Wang, W. Chen, Y. Zhao, T. Yong, L. Gan, H. Xu, X. Yang, Hydrophilicity/hydrophobicity reversible and redox-sensitive nanogels for anticancer drug delivery, *Mol. Pharm.* 12 (2015) 1636–1647.
- [17] A.K.H. Hirsch, F. Diederich, M. Antonietti, H.G. Börner, Bioconjugates to specifically render inhibitors water-soluble, *Soft Matter* 6 (2010) 88–91.
- [18] S. Wiecezorek, E. Krause, S. Hackbarth, B. Röder, A.K.H. Hirsch, H.G. Börner, Exploiting specific interactions toward next-generation polymeric drug transporters, *J. Am. Chem. Soc.* 135 (2013) 1711–1714.
- [19] M. Meißler, A. Taden, H.G. Börner, Enzyme-triggered anti-fouling coatings: Switching bioconjugate adsorption via proteolytically cleavable interfering domains, *ACS Macro Lett.* 5 (5) (2016) 583–587.
- [20] P. Wilke, N. Helfricht, A. Mark, G. Papastavrou, D. Faivre, G.H. Börner, A direct combinatorial strategy towards next generation, mussel-gluce inspired saltwater adhesives, *J. Am. Chem. Soc.* 136 (2014) 12667–12674.
- [21] T. Schwemmer, J. Baumgartner, D. Faivre, H.G. Börner, Peptide-mediated nanoengineering of inorganic particle surfaces: a general route toward surface functionalization via peptide adhesion domains, *J. Am. Chem. Soc.* 134 (2012) 2385–2391.
- [22] R. Gentsch, F. Pippig, S. Schmidt, P. Cernoch, J. Polleux, H.G. Börner, Single-step electrospinning to bioactive polymer nanofibers, *Macromolecules* 44 (2011) 453–461.
- [23] L. Hartmann, H.G. Börner, Precision polymers: monodisperse, monomer-sequence defined segments to target future demands of polymers in medicine, *Adv. Mater.* 21 (2009) 3425–3431.
- [24] H.G. Börner, Strategies exploiting functions and self-assembly properties of bioconjugates for polymer and material sciences, *Prog. Polym. Sci.* 34 (2009) 811–851.
- [25] S. Wiecezorek, S. Vigne, T. Masini, D. Ponader, L. Hartmann, A.K.H. Hirsch, G.H. Börner, Combinatorial screening for specific drug solubilizers with switchable release profiles, *Macromol. Biosci.* 15 (2015) 82–89.
- [26] S. Wiecezorek, T. Schwaar, H.G. Börner, Specific drug formulation additives: revealing the impact of architecture and block length ratio, *Biomacromolecules* 16 (2015) 3308–3312.
- [27] A. Sunder, R. Hanselmann, H. Frey, R. Mülhaupt, Controlled synthesis of hyperbranched polyglycerols by ring-opening multibranching polymerization, *Macromolecules* 32 (1999) 4240–4246.
- [28] R. Haag, F. Kratz, Polymer therapeutics: concepts and applications, *Angew. Chem. Int. Ed.* 45 (2006) 1198–1215.
- [29] M. B.U. Schäfer-Korting, A. Gamer, A. Haberland, E. Haltner-Ukomadu, M. Kaca, H. Kamp, M. Kietzmann, H.C. Korting, H.U. Krächter, C.M. Lehr, M. Liebsch, A. Mehling, F. Netzlaff, F. Niedorf, M.K. Rübbecke, U. Schäfer, E. Schmidt, S. Schreiber, K.R. Schröder, H. Spielmann, A. Vuia, Reconstructed human epidermis for skin absorption testing: results of the German prevalidation study, *Altern. Lab. Anim* 34 (2006) 283–294.
- [30] M. B.U. Schäfer-Korting, W. Diembeck, H.J. Düsing, A. Gamer, E. Haltner-Ukomadu, C. Hoffmann, M. Kaca, H. Kamp, S. Kersen, M. Kietzmann, H.C. Korting, H.U. Krächter, C.M. Lehr, M. Liebsch, A. Mehling, C. Müller-Goymann, F. Netzlaff, F. Niedorf, M.K. Rübbecke, U. Schäfer, E. Schmidt, S. Schreiber, H. Spielmann, A. Vuia, M. Weimer, The use of reconstructed human epidermis for skin absorption testing: results of the validation study, *Altern. Lab. Anim* 36 (2008) 161–187.
- [31] S. Lombardi Borgia, M. Regehy, R. Sivaramakrishnan, W. Mehnert, H.C. Korting, K. Danker, B. Röder, K.D. Kramer, M. Schäfer-Korting, Lipid nanoparticles for skin penetration enhancement—correlation to drug localization within the particle matrix as determined by fluorescence and parelectric spectroscopy, *J. Control. Release* 110 (2005) 151–163.